Earth's Core-Mantle Boundary: Results of Experiments at High Pressures and Temperatures

ELISE KNITTLE* AND RAYMOND JEANLOZ

Laboratory experiments document that liquid iron reacts chemically with silicates at high pressures ($\geq 2.4 \times 10^{10}$ Pascals) and temperatures. In particular, $(Mg,Fe)SiO_3$ perovskite, the most abundant mineral of Earth's lower mantle, is expected to react with liquid iron to produce metallic alloys (FeO and FeSi) and nonmetallic silicates (SiO_2 stishovite and $MgSiO_3$ perovskite) at the pressures of the core-mantle boundary, 14×10^{10} Pascals. The experimental observations, in conjunction with seismological data, suggest that the lowermost 200 to 300 kilometers of Earth's mantle, the D″ layer, may be an extremely heterogeneous region as a result of chemical reactions between the silicate mantle and the liquid iron alloy of Earth's core. The combined thermal-chemical-electrical boundary layer resulting from such reactions offers a plausible explanation for the complex behavior of seismic waves near the core-mantle boundary and could influence Earth's magnetic field observed at the surface.

THE EARTH'S CORE-MANTLE BOUNDARY IS AT A DEPTH OF 2900 km beneath the surface, yet it has a profound influence over the thermal and chemical evolution of the planetary interior. The largest change in bulk composition inside Earth occurs at this boundary, which separates the liquid iron alloy of the outer core from the crystalline silicates of the mantle. As such, it is a dynamic boundary between the rapidly convecting outer core and the slowly convecting mantle, modulating the temperature gradient in the deep Earth. Moreover, the properties of the core-mantle boundary influence, and perhaps control, the propagation of the magnetic field out of the core and the dynamical coupling between the mantle and core (*1–3*).

Most of the direct information about the base of the mantle has come from seismological observations, which reveal it to be a region of complex structure. The core-mantle boundary and the lowermost ~200 to 300 km of the mantle, designated the D″ layer in seismology, exhibits radial and lateral heterogeneity in seismic velocities, anomalous seismic velocity gradients, discontinuities in both shear- and compressional-wave velocities, and strong scattering (*4, 5*). In addition, there may be topography of ~0.1 to 10 km on the core-mantle boundary, and recent observations suggest that there is an anomalous layer at the top of the outer core (Fig. 1) (*6*).

The D″ layer has often been interpreted as a thermal boundary layer, with heat emanating from the core providing an energy source for the general convection of Earth's mantle; also, mantle thermal plumes may originate in the D″ region (7). The surface expression of these two modes of heat transport, convection and plumes, are plate tectonics and hotspots such as the Hawaiian Islands.

The inference that the core-mantle boundary is a thermal boundary layer is supported by recent measurements of the melting temperatures of candidate core components at high pressures. These experiments indicate that core temperatures are likely to be in excess of 4500 K and that the thermal boundary layer at the base of the mantle may have to support radial temperature gradients of 1000 K or more over a depth interval of ~200 km (*8, 9*). The need to maintain a stable thermal boundary layer with such a large temperature gradient, coupled with the seismic observations of extreme heterogeneity, suggests that the D″ region is also a chemical boundary layer between the mantle and the core. That is, compositional density variations may be required to counteract the thermal buoyancy forces that reduce the temperature gradient by advection. Several mechanisms for developing chemical heterogeneities in the D″ layer have been proposed, including the accumulation of subducted slabs at the base of the mantle (*2, 10*) or a phase change in the silicate components of the lower 200 km of the mantle (*11–14*).

Earlier experimental work has demonstrated that, at the pressures of the silicate perovskite stability field (>24 GPa, the pressure at ~670 km depth), molten iron reacts with crystalline silicate perovskite (*15, 16*). The evidence for such chemical reactions includes visual observations and x-ray diffraction measurements, which show that the products of iron reacting with $Mg_{0.88}Fe_{0.12}SiO_3$ perovskite are SiO_2 in the high-pressure stishovite polymorph [or a closely related phase (*14*)], end-member $MgSiO_3$ perovskite, nonstoichiometric $Fe_{0.9}O$ wüstite (or $Mg_{0.1}Fe_{0.9}O$ magnesiowüstite), and an Fe_xSi_y alloy where x and y are uncertain.

These results from diamond-cell experiments lead to the intriguing possibility that chemical reactions also take place at the boundary between Earth's silicate mantle and liquid iron core. Thus, the motivation of the experimental work we describe in this article was to explore the chemical and mineralogical nature of the D″ layer and the core-mantle boundary. Specifically, we investigated the possibility that chemical reactions between molten iron and crystalline silicates lead to the development of a chemical boundary layer at the base of the mantle, and to the contamination (alloying) of Earth's liquid outer core. To accomplish this, we have attempted to recreate

The authors are in the Department of Geology and Geophysics, University of California, Berkeley, CA 94720.

*Present address: Earth Sciences Board, University of California, Santa Cruz, CA 95064.

Table 1. Sample descriptions. The designations "u" and "m" indicate that the microprobe traverses were taken across unmelted and melted edges, respectively. Average pressures are reported as determined from ruby fluorescence in the silicate material away from the iron edge. Our estimated uncertainty of the pressure at the iron-silicate interface is approximately 15%.

Sample	Pressure (GPa)	Comments
70-1u	≥70	No melting at interface
20m	~20	Iron foil melted at interface
70-2m	≥70	Iron foil melted at interface
70-3m	≥70	Iron foil melted at interface
75m	≥75	Iron foil melted at interface
70-1m	≥70	Iron foil melted at interface

the core-mantle boundary in miniature, within a 200-μm diameter sample inside the laser-heated diamond cell. We then use the electron microprobe to analyze the compositional variations across the reaction zones that are produced between iron and silicate perovskite at elevated pressures and temperatures.

Experimental Results

The high pressure-temperature conditions achieved in our experiments were generated using Mao-Bell–type diamond cells and laser heating (*17, 18*). The samples consisted of iron foils embedded in a silicate perovskite matrix with a composition representative of Earth's lower mantle. The laser was used to melt the iron foil without melting the silicate as is representative of the core-mantle boundary. Four separate samples were heated to greater than 3500 K at average pressures in excess of 70 GPa (Table 1). In addition, two samples were used for comparison: an unheated sample taken to pressures exceeding 70 GPa and a sample that was reacted at a pressure near 20 GPa. This latter pressure is below that at which the $Mg_{0.88}Fe_{0.12}SiO_3$ orthopyroxene starting material converts to the perovskite structure.

Reaction zones between the iron and silicate were observed in all four samples at the interfaces where the iron foil melted. As is evident from Fig. 2, the reaction zone was characterized in transmitted light by blurring of the iron-silicate boundary. However, the edge between the foil and silicate was sharp and clearly identifiable in reflected light. Hence the blurring was not due to shredding or small-scale mechanical intermixing of the iron and silicate. Instead, we attribute the apparent darkening of the reaction zone within the silicate, as observed in transmitted light, to the penetration and diffusion of a small amount of iron out of the foil and into the silicate, as described below.

Electron microprobe analyses of the unreacted contact at ≥70 GPa (sample 70-1u) provide a resolution test for our technique and a basis for interpreting the scale and nature of the reaction zone (*19*). The edge between the silicate and the iron foil was sharply resolved in the compositional profile; these data indicate that the microprobe analyses have a spatial resolution less than the step spacing of 2 μm (Fig. 3). The chemical analyses of the silicate give a stoichiometry of $(Mg_{0.88}Fe_{0.12})SiO_3$, in good agreement with analyses of the starting material.

One representative microprobe traverse for the four major elements, Mg, Fe, Si, and O, in a reacted edge in sample 70-3m is plotted in Fig. 4. In contrast with the unreacted edge, a compositional gradient is observed on both sides of the iron-silicate interface, and O, S, and Mg had diffused into the melted (now quenched) foil, whereas Fe had diffused into the silicate.

To highlight the compositional gradients at the boundary between iron and silicate as a function of pressure, we subtracted the weight percentages of Mg, Fe, Si, and O for the unreacted edge (sample 70-1u) from the values for each of the five reacted edges. The result is a plot showing the change in the compositional profile due to the iron-silicate reaction (Figs. 5 to 7), and the distance

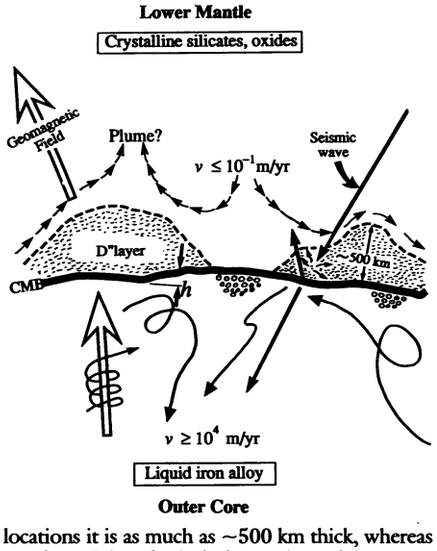

Fig. 1. Summary of geophysical observations characterizing the core-mantle boundary (CMB) and nearby regions (*1–6*). Examination of amplitudes and travel times of seismic waves indicates that the boundary may have topography of magnitude $h \sim 0.1$ to 10 km, and that it is overlain by an anomalous region (D" layer, shown stippled) that is ~200 to 300 km thick, on average. The D" layer is extremely heterogeneous in physical properties, as indicated by strong scattering that is observed for seismic waves (shown schematically), and it appears to vary in thickness: in some locations it is as much as ~500 km thick, whereas in other locations it is not evident. Seismological observations also suggest that the outermost core may locally be anomalous (open circle pattern below the CMB). The geomagnetic field (open arrows) is produced by magnetohydrodynamic processes involving the turbulent flow of the liquid iron alloy making up the outer core (shown schematically by long arrows). The flow velocity of $\sim 10^4$ m/yr, or more, in the outer core is estimated from the rate of change of the magnetic field observed at Earth's surface and is much greater than the velocity of mantle convection, $\leq 10^{-1}$ m/yr (short arrows), that is obtained from the rate at which tectonic plates move at the surface. Mantle plumes, creating hot spots observed at Earth's surface, may originate in or above the D" layer.

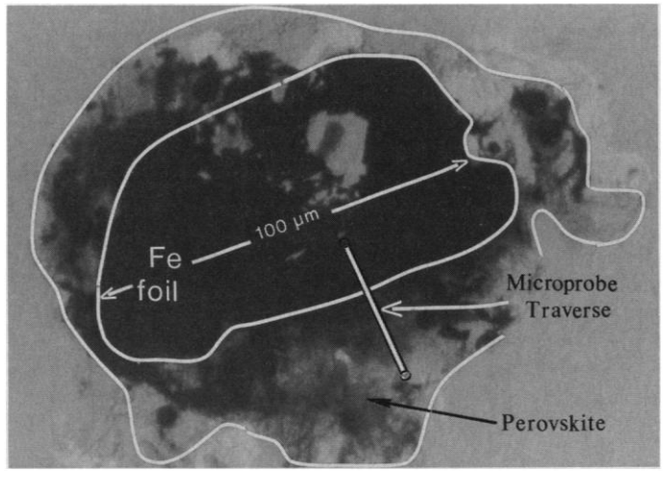

Fig. 2. Photograph of an iron foil reacted with silicate perovskite (sample 70-3m) and prepared for analysis in the electron microprobe, as seen in transmitted light. The iron foil is outlined in white and is about 100 μm in diameter. The outer white line indicates the extent of the silicate surrounding the iron foil. The dark regions outside the foil are zones where the inside edge of the foil was melted with the laser, and the molten iron reacted with the silicate perovskite. The white line indicates the microprobe traverse for this sample; its length is representative of all the traverses measured. In all cases, data were collected at 2-μm intervals from the iron foil through the reacted zone and to a pristine region in the silicate perovskite.

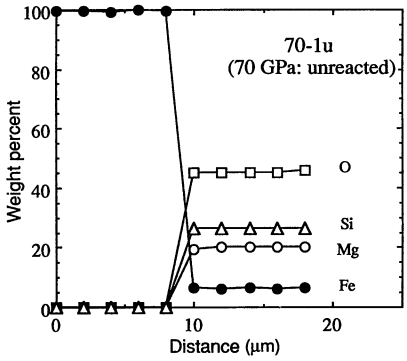

Fig. 3. Amount (in weight percent) of O, Si, Mg, and Fe as a function of distance in sample 70-1u. Composition was obtained at 2-μm steps across an unreacted edge (located at 9 ± 1 μm) between the iron foil and silicate perovskite. The silicate composition that is measured corresponds to $Mg_{0.88}Fe_{0.12}SiO_3$.

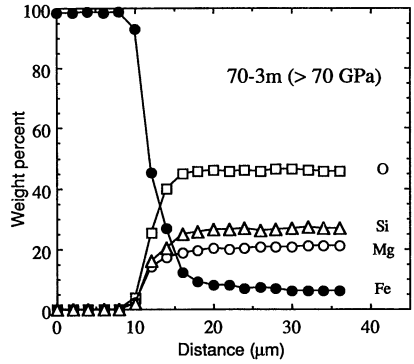

Fig. 4. Representative example of the chemical gradient observed across the interface between perovskite and a melted iron foil (sample 70-3m). The iron-silicate interface is at ~13 μm.

ranges plotted in these figures are determined by the length of the compositional profile measured for sample 70-1u (9 μm into the silicate from the edge of the foil, and >10 μm into the iron foil).

For sample 20m heated at 20 GPa, O, Mg, and Si had migrated into the iron foil, but only over a distance that is barely resolvable by our analyses: within 2 (±1) μm inside the iron-silicate boundary. Beyond this point, no measurable amounts of either O, Mg, or Si were observed in the iron. In comparison, the migration of these elements was greater in the samples reacted at higher pressures (Fig. 6). Specifically, O was clearly present at 7 (±2) μm, and Mg and Si were present at 4 (±1) μm into the iron foil.

On the silicate side of the iron-perovskite boundary, Fe was enriched over a distance of at least 12 to 15 μm in the samples reacted at ≥70 GPa (Fig. 7). This enrichment of Fe is what gives the sample its darkened appearance in the reacted region (Fig. 2). In comparison, the amount of Fe observed in the silicate from the 20 GPa experiment was uniform up to a distance within 3 (±1) μm of the interface; this composition is exactly that expected from the silicate starting material.

The same point is illustrated in Fig. 8, where the enrichment of Fe into the silicate is expressed as the molar ratio of Mg to Fe. This ratio is ideally 7.33 for $(Mg_{0.88}Fe_{0.12})SiO_3$ perovskite, as exhibited by the unreacted sample within 1μm of the edge of the iron foil. Similarly, the 20 GPa reacted edge attained the ideal Mg/Fe ratio within 3 (±1) μm of the foil. Note that the silicate in sample 20m has an Mg/Fe ratio of 6.85, corresponding to a perovskite of composition $(Mg_{0.873},Fe_{0.127})SiO_3$, because of variations in the iron content of the natural starting material that we have used.

The penetration of Fe for at least 12 to 15 μm into the silicate, at ≥70 GPa, is particularly interesting in that these samples were not melted on the silicate side of the interface. Hence, the enrichment of Fe in the silicate may have been the result of liquid metal migrating along the perovskite grain boundaries by means of a surface-tension mechanism (*9, 20*). Alternatively, the penetration of Fe into the silicate may reflect a type of Soret diffusion, in which the heaviest component of a chemical system (in this case Fe) migrates down the temperature gradient: that is, away from the laser-heated spot. Soret diffusion has been previously observed in diamond-cell experiments using laser heating (*18*).

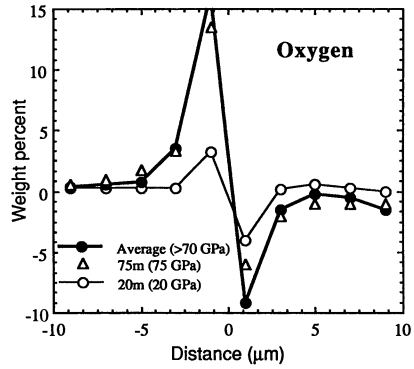

Fig. 5. Expanded view of the distribution of O across the iron-silicate interface for all samples in which the foil was melted (the foil and silicate lie at negative and positive distances, respectively). The results are shown as deviations from the compositional profile measured across the unreacted sample interface (70-1u). Positive or negative deviations in weight percent represent enrichment or depletion of O. The solid circles are the average values for all four samples that were reacted at high pressures (samples 70-1m, 70-2m, 70-3m, and 75m). For comparison, an individual profile is shown for sample 75m (open triangles). Finally, the open circles are the values for the interface reacted at ~ 20 GPa (sample 20m).

Implications for the Core-Mantle Boundary

Our experimental results have implications for several aspects of the core-mantle boundary system, in particular (i) the development of chemical heterogeneities in the D″ layer, and (ii) the possibility that chemical reactions at the core-mantle boundary provide a mechanism for the incorporation of light-alloying components into Earth's outer core.

The thermodynamic driving force that causes liquid iron to react chemically with silicate perovskite in our experiments and, by implication, at the core-mantle boundary can be examined as follows. On the basis of primarily our earlier experimental results (*15, 16*), we propose the following balanced equation for the chemical reaction between liquid iron and silicate perovskite at high pressure:

$$Mg_xFe_{1-x}SiO_3 + 3[(1-x) - s]Fe = xMgSiO_3 + sSiO_2 + [3(1-x) - 2s]FeO + [(1-x) - s]FeSi$$

Here x is the proportion of Mg component in the unreacted perovskite and s is the number of moles of stishovite produced in the reaction. The constraint that $0 \le s \le 1 - x$ applies because both SiO_2 (stishovite or a closely related phase) and FeSi alloy are observed as reaction products.

A unique solution is obtained if we assume that the amounts of FeSi and SiO_2 produced in the reaction are the same. Our experimental results are consistent with this assumption, although we cannot quantify the relative amounts of FeSi and SiO_2 produced to better than a factor of 2 to 5. Thus, with $x \approx 0.9$, the reaction pertaining to our data is:

$$Mg_{0.9}Fe_{0.1}SiO_3 + 0.15\ Fe = 0.90\ MgSiO_3 + 0.20\ FeO + 0.05\ FeSi + 0.05\ SiO_2 \quad (1)$$

The thermochemical properties of these phases are not known sufficiently well to evaluate quantitatively the heat of this reaction. However, we can determine the sign of the thermodynamic driving force by calculating the volume change upon reaction for the minerals as a function of pressure at 300 K. We ignore the effects of temperature because they are small relative to the pressure effects and are poorly constrained. Qualitatively, we expect temperature to affect the volume change, by way of thermal expansion, in a manner

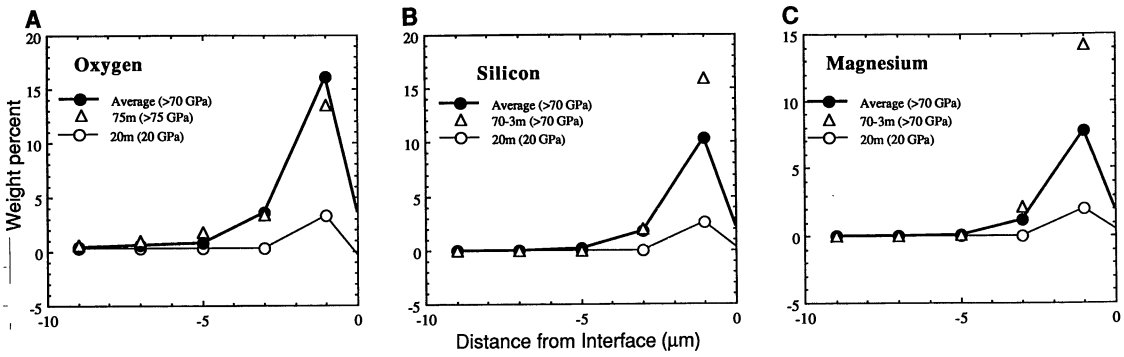

Fig. 6. Compositional profiles for O (**A**), Mg (**B**), and Si (**C**) into the iron, for samples in which the foil was melted. The axes and symbols have the same meanings as in Fig. 5, except that sample 70-3m (rather than sample 75m) is shown for comparative purposes in (B) and (C).

opposite to that of pressure, but to a much smaller degree. Furthermore, entropy may favor this reaction, driving it to the right.

The parameters used for the calculation are given in Table 2. The molar volumes (V_0) at high pressure were determined with a third-order Birch-Murnaghan equation of state (*21*). We use the values for the solid α-phase of Fe in our calculation: as molten Fe would be expected to have a larger molar volume than the solid, this represents a conservative estimate of the molar volume change (ΔV) of reaction at 300 K. Additionally, at high pressures the liquidus phase of Fe is probably the face-centered cubic γ-phase. At the pressure of the core-mantle boundary, 136 GPa, the molar volumes of α- and γ-iron are within ~4% of each other at 300 K. Therefore, our use of the properties of α-iron yields a lower bound on the volume of iron, hence the $|\Delta V|$ of reaction, at all pressures considered.

In addition to calculating ΔV as a function of pressure, we also explored the effect of greater Fe content (up to $x = 0.8$) in the silicate perovskite reactant. The results (Fig. 9) show that the reaction is thermodynamically favored at high pressures; that is, the ΔV of reaction is negative under all pressure-composition conditions examined, and higher pressure and greater Fe content in the silicate perovskite tend to drive the reaction.

This analysis is compatible with all of our experimental observations and suggests that chemical reactions must inevitably take place at the core-mantle boundary. Such reactions may have a profound effect on the physical properties of D″, particularly because our experiments show that major compositional heterogeneities, consisting of iron alloys ($Fe_{0.9}O$ and FeSi) mixed with silicates ($MgSiO_3$ and SiO_2), are likely to be present at the base of the mantle. Variations in the proportions of these metal and silicate phases can produce strong heterogeneity, not only in density and elastic properties (see Table 2) but also in the electrical conductivity. Specifically, the silicates produced in the reaction have electrical conductivities characteristic of poor semiconductors, $\sigma \leq 10^{-2}$ S/m, and the iron alloys FeO and FeSi have conductivities close to that of Fe ~ 10^6 S/m (*16, 22*). Hence, the electrical conductivity in the D″ layer may vary spatially by as much as eight orders of magnitude.

The hypothesis that heterogeneities are formed by chemical reactions at the core-mantle boundary is consistent with a wide variety of geophysical observations (Fig. 1). Both radial and lateral variations in seismic wave velocity and scattering of seismic waves near the core-mantle boundary may result from chemical heterogeneities having strong density or velocity contrasts, such as those implied by Table 2 (Fig. 10).

Our experiments cannot provide a length scale for such heterogeneities. Indeed, the size of the heterogeneities depends on a number of factors, including the extent of chemical reaction at the core-mantle boundary, the amount of convective mixing in the D″ region due to strong internal temperature gradients, and the extent of interaction of mantle convection with the chemical layer. However, some studies have indicated that the scattering of seismic waves in the D″ layer can best be explained by heterogeneities less than 100 km in diameter (*5, 23*).

We infer that there are two important time scales, and correspondingly two length scales, for the development of heterogeneities at the base of the mantle due to chemical reaction with the core (Fig. 10). First, the mantle rock that is directly in contact with the outer-core liquid is likely to react rapidly, instantaneously in terms of geological time, as is observed in our experiments. Presumably, the reaction zone penetrates upward only on the order of ~10^1 to 10^2 m, corresponding to plausible lengths for capillary rise along grain boundaries in the mantle (*9*). Recent VLBI observations may have identified the presence of such a reaction zone extending a few hundred meters into the mantle above the core (*24*).

But on the longer time scale of mantle convection, at rates typical of plate tectonics (~10^{-2} to 10^{-1} m/yr) for example, this reaction zone is swept upward into the mantle, and fresh rock is exposed to the core liquid. Because of its increased density, relative to unreacted mantle rock, the alloy-silicate mixture cannot rise far into the mantle, and we infer that this heterogeneous accumulation of reaction products is what makes up the D″ layer (*2, 25*). In particular, the

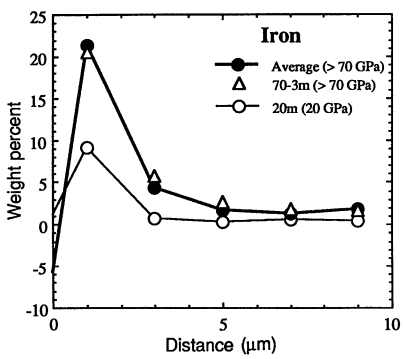

Fig. 7. Compositional profile of Fe into the silicate perovskite for samples in which the foil (at negative distance) was melted. The axes and symbols have the same meaning as in Fig. 5, except that sample 70-3m (rather than 75m) is shown for comparative purposes.

Fig. 8. Molar ratios of Mg to Fe as a function of distance from the iron-silicate interface. The closed circles indicate the results for the unreacted sample edge [sample 70-1u, with composition $(Mg_{0.88}Fe_{0.12})SiO_3$], whereas the open circles give the results for the sample reacted at 20 GPa [20m, with composition $(Mg_{0.873}Fe_{0.127})SiO_3$]. The open triangles are the average values for all of the samples reacted at high pressures.

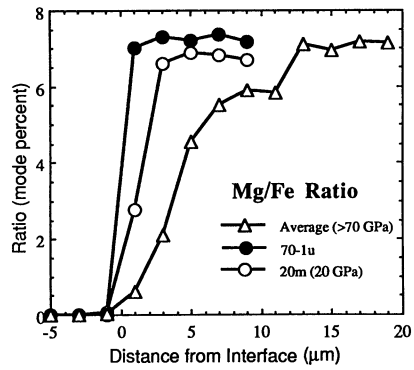

Table 2. Properties of core-mantle boundary materials at zero pressure and 300 K. K_T is the bulk modulus at constant temperature; pv, perovskite; hpp, high-pressure phase.

Composition	V_0 (cm³/mol)	K_T (GPa)	dK_T/dP
$Mg_{1-x}Fe_xSiO_3$ (pv)	(24.46 ± 0.04) + (1.03 ± 0.28)X_{Fe} (*26*)	266 ± 6 (*13*)	3.9 ± 0.4 (*13*)
Fe (α-phase)	7.092 ± 0.004 (*27*)	167 ± 2 (*28*)	5.3 ± 0.6 (*28*)
SiO_2 (stishovite)	14.01 ± 0.01 (*26*)	314 ± 10 (*29*)	4 ± 2 (*26*)
$Fe_{0.9}O$ (hpp)	10.95 ± 0.27 (*11*)	195 ± 10 (*11*)	4 ± 1*
FeSi (cubic)	13.35 ± 0.18 (*30*)	180 ± 10 (*31*)	4 ± 1*

*Estimated

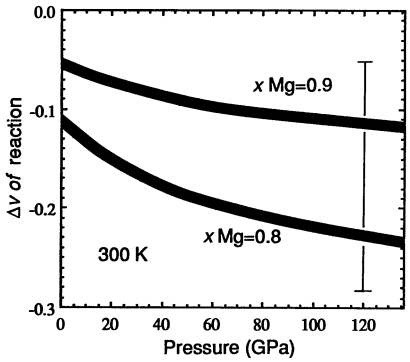

Fig. 9. Volume decrease at 300 K for the chemical reaction describing our experiments, shown as a function of pressure up to 136 GPa. The molar proportion of magnesium to Fe + Mg components in the perovskite prior to reaction is indicated by *x*.

lowermost mantle would consist of partially entrained reaction products that have been stirred with the mantle rock on length scales ≤100 km. On the core side, we presume that the products of reaction with the mantle (primarily O alloying with Fe) are swept downward by the rapid, turbulent flow of the outer-core liquid: the same flow that produces the geomagnetic field.

Thus, one implication of a heterogeneous, chemically reacted D″ layer applies to the propagation of Earth's magnetic field from the core into the mantle. That is, because the electrical conductivity of the D″ region should be extremely heterogeneous, the magnetic field lines emanating from the core would become deflected, because of induction, by the metallic heterogeneities at the bottom of the mantle. The field lines can only penetrate through the metal-rich heterogeneities within time periods of magnetic diffusion (10^1 to 10^2 years) (*9*). In detail, the magnetic diffusion time depends on the size and distribution of the heterogeneities. However, this effect may account for some of the secular variation of Earth's magnetic field, which occurs on comparable time scales.

Implications for the Composition of the Outer Core

The solubility of oxide components into molten iron at high pressures suggests that chemical reactions between the core and the mantle may be an important process affecting the composition of Earth's outer core over geological time. The observation that both Si and O form metallic alloys with Fe at high pressure (FeO and FeSi) (*15*) means that they are plausible core constituents. Thus, either may account for why the liquid outer core is ~10% less dense than pure Fe, and hence must contain a light alloying component, and yet behaves as a single-phase, metallic Fe alloy.

The experiments show that O is far more soluble in liquid Fe at high pressures than either Si or Mg. One implication of our experiments is that O is inevitably present in Earth's outer core, regardless of the detailed composition and state of the core after it was formed. However, it is noteworthy that the other two major components of mantle silicates, Mg and Si, have measurable solubility in liquid Fe at high pressures. If the outer core attained some of its present composition by chemical reactions at the core-mantle boundary, it may contain a number of different contaminants. Nevertheless, based simply on its relative abundance in the mantle, as well as our experimental observations, O is favored as a major core component.

It is tempting to estimate the diffusion lengths for O, Si, and Mg in molten iron from our experiments, and extrapolate the data to core conditions. However, due in particular to the large temperature gradients around the laser-heated spot, it is currently not possible to apply quantitatively the penetration length scales from the experimental compositional profiles to processes deep in Earth. For example, the time over which the iron foil is melted in these experiments is 1 to 10 min, and the O is incorporated 7 (±2) μm into the foil. If considered literally to represent a diffusion length of O in iron at high pressure, these results imply that over the age of Earth, O would have diffused only about 1 km into the outer core.

In reality, the outer core is a vigorously convecting system, such that O (and Si and Mg) could be incorporated into the outer core rapidly and efficiently. Indeed, the recently observed seismic velocity anomalies at the top of the outer core might well represent the products of reaction with the overlying mantle. Thus, it may be that the entire budget of light alloying component in the outer core has come from chemical reactions with the mantle and that such processes are continuing at present. That is, the composition of the core may be evolving throughout geological time.

Conclusions

Our preferred model of the core-mantle boundary and the D″ region of Earth, as suggested by experimental results at ultrahigh pressures and temperatures, consists of vigorous chemical reactions taking

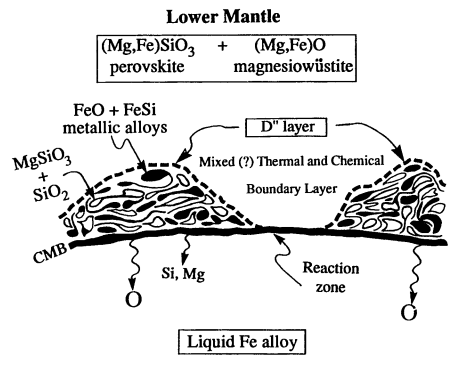

Fig. 10. Structure of the core-mantle boundary (CMB) and D″ region, as suggested by geophysical and experimental observations. A reaction zone, ~10^1 to 10^2 m thick, is rapidly created at the interface between the mantle and core (*9, 15*). Mantle components (O and lesser amounts of Si and Mg) are dissolved into the outer core and rapidly dispersed by the turbulent flow of the liquid iron alloy. On time scales ≥10^7 years, the reaction zone at the CMB is entrained by the large-scale convective flow of the mantle (Fig. 1), but cannot be raised far upward (> ~100 to 500 km) because of the high density of the reaction products relative to the mantle (*9, 25*). The resulting mixture of unreacted mantle and of heterogeneous reaction products makes up the ~200- to 300-km-thick D″ layer, which includes metallic alloys (shown as dark blobs) and relatively insulating silicates (shown as open blobs).

place between the liquid iron alloy of the outer core and the crystalline silicates of the mantle. These reactions dissolve components of the mantle, particularly O, into Earth's outer core and thereby contribute to the budget of light elements alloyed with the liquid Fe. On the mantle side of the boundary, some Fe may be drawn from the core into the D″ region by a surface-tension driven, capillary process. The resulting chemical reactions break down the silicate perovskite to form iron alloys and dense silicates, including stishovite or a closely related phase. These reaction products could then form a discrete region in the ~200 to 300 km above the core-mantle boundary. The large differences in physical properties among reaction products, the silicate- and iron-rich regions that we propose occur in the D″ layer, are in accord with the seismological and geomagnetic observations of the presence of a complex, heterogeneous zone at the bottom of the mantle.

REFERENCES AND NOTES

1. J. Bloxham and D. Gubbins, *Nature* **317**, 777 (1985); D. Gubbins and M. Richards, *Geophys. Res. Lett.* **13**, 1521 (1986); D. E. Loper and K. McCartney, *ibid.*, p. 1525; J. Bloxham and D. Gubbins, *Nature* **325**, 511 (1987); J. Bloxham, *Geophys. Res. Lett.* **15**, 185 (1988); P. Olson, *ibid.* **16**, 613 (1989).
2. G. F. Davies and M. Gurnis, *Geophys. Res. Lett.* **13**, 1521 (1986).
3. B. A. Buffet, T. A. Herring, P. M. Mathews, I. I. Shapiro, *Eos* **71**, 496 (1990).
4. S. S. Alexander and R. A. Phinney, *J. Geophys. Res.* **71**, 5943 (1966); I. S. Sacks, *ibid.*, p. 1173; H. Kanamori, *ibid.* **72**, 558 (1967); I. S. Sacks, *ibid.*, p. 2589; G. G. Buchbinder, *ibid.* **73**, 5901 (1968); I. S. Berzon, S. D. Kogan, I. P. Passechnik, *Earth Planet. Sci. Lett.* **16**, 166 (1972); C. Wright, *J. Geophys. Res.* **78**, 4965 (1973); B. Mitchell and D. V. Helmberger, *ibid.*, p. 6009; J. R. Cleary, *Phys. Earth Planet. Inter.* **9**, 13 (1974); A. M. Dziewonski and R. A. W. Haddon, *ibid.*, p. 28; G. Müller, A. H. Mula, S. Gregersen, *ibid.* **14**, 30 (1977); A. C. Chang and J. R. Cleary, *ibid.* **24**, 15 (1981); A. M. Dziewonski and D. L. Anderson, *ibid.* **25**, 297 (1981); L. J. Ruff and D. V. Helmberger, *ibid.* **26**, 181 (1982); T. Lay and D. V. Helmberger, *Geophys. J. R. Astron. Soc.* **75**, 799 (1983); *J. Geophys. Res.* **88**, 8160 (1983); D. J. Doornbos, *ibid.*, p. 3490; B. A. Bolt and M. Niazi, *Geophys. J. R. Astron. Soc.* **79**, 825 (1984); V. Cormier, *J. Geophys.* **57**, 14 (1985); D. J. Doornbos, S. Spiliopoulos, F. D. Stacey, *Phys. Earth Planet. Inter.* **39**, 28 (1986); T. Lay and C. J. Young, *J. Geophys.* **59**, 11 (1986); W. Menke, *Geophys. Res. Lett.* **13**, 1501 (1986); C. J. Young and T. Lay, *Annu. Rev. Earth Planet. Sci.* **15**, 25 (1987); K. Bataille and Flatté, *J. Geophys. Res.* **93**, 15057 (1988); E. Garnero, D. Helmberger, G. Engen, *Geophys. Res. Lett.* **15**, 609 (1988); I. S. Sacks, J. A. Snoke, L. Beach, *Geophys. J. R. Astron. Soc.* **59**, 379 (1989); D. Baumgardt, *Geophys. Res. Lett.* **16**, 657 (1989); M. E. Wysession and E. A. Okal, *ibid.*, p. 1417; M. Weber and J. P. Davis, *Geophys. J. Int.* **102**, 231 (1990); C. J. Young and T. Lay, *J. Geophys. Res.* **95**, 17385 (1990); J. P. Davis and M. Weber, *Geophys. Res. Lett.* **17**, 187 (1990).
5. E. M. Laveley, D. Forsyth, P. Friedemann, *Geophys. Res. Lett.* **13**, 1505 (1986).
6. K. C. Creager and T. H. Jordan, *ibid.*, p. 1497; T. Lay and C. J. Young, *ibid.* **17**, 2001 (1990); A. Morelli and A. M. Dziewonski, *Nature* **325**, 678 (1987); A. Souriau and G. Poupinet, *Geophys. Res. Lett.* **17**, 2005 (1990).
7. G. M. Jones, *J. Geophys. Res.* **82**, 1703 (1977); R. Jeanloz and F. M. Richter, *ibid.* **84**, 5497 (1979); D. Yuen and W. R. Peltier, *Geophys. Res. Lett.* **7**, 625 (1980); F. D. Stacy and D. E. Loper, *Phys. Earth Planet. Inter.* **33**, 45 (1983); K. A. Whaler, *Geophys. J. R. Astron. Soc.* **86**, 563 (1986); P. Olson, G. Schubert, C. Anderson, *Nature* **327**, 409 (1987).
8. Q. Williams, R. Jeanloz, J. Bass, B. Svendsen, T. J. Ahrens, *Science* **236**, 181 (1987); Q. Williams, E. Knittle, R. Jeanloz, *J. Geophys. Res.* **96**, 2171 (1991); Q. Williams and R. Jeanloz, *ibid.* **95**, 19299 (1990); E. Knittle and R. Jeanloz, *ibid.*, in press.
9. R. Jeanloz, *Annu. Rev. Earth Planet Sci.* **18**, 357 (1990).
10. L. Ruff and D. L. Anderson, *Phys. Earth Planet. Inter.* **21**, 181 (1980).
11. R. Jeanloz and T. J. Ahrens, *Geophys. J. R. Astron. Soc.* **62**, 505 (1980).
12. This mechanism appears unlikely for the silicate perovskite component of the mantle [compare with (*13*)].
13. E. Knittle and R. Jeanloz, *Science* **235**, 668 (1987).
14. Recent work suggests that SiO_2 stishovite distorts to a $CaCl_2$ structure at the pressures of the core-mantle boundary [Y. Tsuchida and T. Yagi, *Nature* **340**, 217 (1989); R. Jeanloz, *ibid.*, p. 184]. As this distorted structure has the same volume as stishovite, we use the properties of stishovite in this analysis.
15. E. Knittle and R. Jeanloz, *Geophys. Res. Lett.* **13**, 1541 (1986).
16. ———, *ibid.* **16**, 609 (1989).
17. Samples of 25-μm-thick iron foil (source: Alfa-Ventron, Danvers, MA) of typical dimensions 50 to 100 by 50 to 100 μm were completely surrounded by enstatite and compressed in a Mao-Bell–type diamond cell. The enstatite starting material is a natural sample from Bamble, Norway, with an average composition of $(Mg_{0.88}Fe_{0.12})SiO_3$ (*13*) that varies by <1% in Mg/Fe ratio. A few grains of ruby were added to the silicate region of the sample to act as a pressure calibrant [H. K. Mao, P. M. Bell, J. W. Shaner, D. J. Steinberg, *J. Appl. Phys.* **49**, 3276 (1978)]. Four were compressed to average pressures in excess of 70 GPa, and one experiment was performed at 20 GPa for comparison with the ultrahigh pressure results. The silicate surrounding the iron foil was converted to the high-pressure perovskite structure by heating with a CW Nd:YAG laser (1064 nm wavelength, focal diameter of 20 to 25 μm and ≤25 W in TEM_{00} mode) at low power, such that temperatures remained well below the melting points of both iron and the silicate [~1800 to 2000 K: (*18*); E. Knittle and R. Jeanloz, *Geophys. Res. Lett.* **16**, 421 (1989)]. Subsequently, the laser beam was focused on the iron foil just inside the edge, where the foil is in contact with the perovskite. The laser power was increased until the foil was melted. In these experiments, it was possible to melt the foil and avoid melting the perovskite because the diameter of the laser beam is much smaller than the size of the foil.
18. D. L. Heinz and R. Jeanloz, *J. Geophys. Res.* **92**, 11437 (1987).
19. After the iron foil and silicate were reacted, the sample was quenched first in temperature and then in pressure. It was then mounted in epoxy and polished for analysis with the electron microprobe. Samples were chosen for study if the polished edge of the iron foil was coincident in both transmitted and reflected light; otherwise, some silicate material could remain on the top surface of the foil and contaminate the analysis. Although there may have been silicate present beneath the foil, it would not tend to contaminate the analysis because of the absorption of both the electron beam and the characteristic x-rays by the overlying iron. The reproducibility of our results between different experiments supports our conclusion that contamination was not a problem. In addition, reacted edges were not studied if the laser beam had melted the silicate perovskite at the edge of the foil. Melting of the silicate could easily be detected by the presence of glassy, round quenched structures, commonly enriched in iron, and located within the silicate. These quenched structures, obliterated the interface between the iron foil and the silicate. An additional problem was the occasional shredding of iron from the foil, which resulted in small (<10 μm) shards of iron embedded in the perovskite near the edge of the foil; this could easily be recognized and avoided, however.

    Samples prepared in this way were examined with an 8-channel ARL electron microprobe operated at an accelerating voltage of 15 kV. Compositional analyses for Mg, Fe, Al, Si, Ca, and O were taken at 2-μm steps across the iron-silicate interface. The steps were planned so as not to straddle the boundary, but to fall either on one side or the other of the interface. The microprobe data were reduced with Bence-Albee correction factors [A. E. Bence and A. L. Albee, *J. Geol.* **76**, 382 (1968)]. Runs were defined as successful if each point taken at a 2-μm interval yielded a weight percent total of 95 to 100%. Some runs had lower totals (and were thus disregarded) because the samples were too thin to provide a proper excitation volume for the particular element being analyzed. The most common reason for this was poor sample preparation. If the decompressed samples (typically 25 to 30 μm in thickness) were mounted in the epoxy at a slight angle, this could result in nonuniform thinning of the sample during polishing. For each run that yielded acceptable results, the microprobe traverse was repeated in order to estimate the uncertainty of the measurement. The measured sample compositions were reproducible to 1 to 2% for Mg, Fe, and Si, and to 5 to 8% for O.
20. D. J. Stevenson, *Geophys. Res. Lett.* **13**, 1169 (1986).
21. F. Birch, *J. Geophys. Res.* **83**, 1257 (1978).
22. R. N. Keeler and A. C. Mitchell, *Solid State Commun.* **7**, 271 (1969); G. Matassov, *LLNL Publ. UCRL-52322* (1977); E. Knittle, R. Jeanloz, A. C. Mitchell, W. J. Nellis, *Solid State Commun.* **59**, 513 (1986); X. Li and R. Jeanloz, *Geophys. Res. Lett.* **13**, 1075 (1987); *J. Geophys. Res.* **95**, 5067 (1990).
23. K. Bataille and S. Flatté, *J. Geophys. Res.* **93**, 15057 (1988).
24. Modeling of the Earth's forced nutations observed by very-long baseline interferometry (VLBI) suggests the presence of an electromagnetic coupling between the mantle and core which can be explained by the presence of an electrically conducting region, corresponding to our reaction zone, in the lowermost ~500 m of the mantle (*3*).
25. N. Sleep, *Geophys. J.* **95**, 437 (1988); U. Hansen and D. A. Yuen, *Nature* **334**, 237 (1988); *Geophys. Res. Lett.* **16**, 629 (1989).
26. R. Jeanloz and A. B. Thompson, *Rev. Geophys. Space Phys.* **21**, 51 (1983).
27. R. Robie, P. Bethke, K. Beardsley, *U.S. Geol. Surv. Bull 1248* (1981).
28. M. W. Guinan and D. N. Beshers, *J. Phys. Chem. Solids* **29**, 541 (1968).
29. D. J. Weidner, J. D. Bass, A. E. Ringwood, W. Sinclair, *J. Geophys. Res.* **87**, 4740 (1982).
30. JCPDS card 22-632.
31. S. P. Marsh, Ed., *LASL Shock Hugoniot Data* (Univ. of California Press, Berkeley, 1980), p. 205.

32. This work was supported by the National Aeronautics and Space Administration. We thank J. Bloxham, B. A. Buffett, L. H. Kellogg, T. Lay, D. J. Stevenson, D. Yuen, and the reviewers for helpful comments and discussion.